

Reactivity of [M(C \wedge P)(S₂C-R)] (M = Pd, Pt; C \wedge P = CH₂-C₆H₄-P(*o*-tolyl)₂-κC,P; R = NMe₂, OEt) toward HgX₂ (X = Br, I). X-ray Crystal Structures of [Pt{CH₂-C₆H₄P(*o*-tolyl)₂-κC,P}(S₂CNMe₂)HgI(μ-I)]₂ and [PdBr(S₂COEt){μ-P(*o*-tolyl)₂-C₆H₄-CH₂-}HgBr]·0.5HgBr₂·C₂H₄Cl₂

Larry R. Falvello, Juan Forniés,* Antonio Martín, Rafael Navarro, Violeta Sicilia, and Pablo Villarroya

Departamento de Química Inorgánica, Instituto de Ciencia de Materiales de Aragón, Universidad de Zaragoza-CSIC, Facultad de Ciencias, E-50009 Zaragoza, Spain

Received May 15, 1997[⊗]

The reaction of the complexes [Pt(C \wedge P)(S₂C-R)] (C \wedge P = CH₂-C₆H₄-P(*o*-tolyl)₂-κC,P, R = NMe₂, OEt) with an equimolar amount of HgX₂ (X = Cl, Br) gives the tetranuclear derivatives [Pt(C \wedge P)(S₂C-R)HgX(μ-X)]₂ [R = NMe₂, X = Br (**3**), I (**4**); R = OEt, X = Br (**5**), I (**6**)] containing Pt→Hg donor–acceptor bonds. The reaction of [Pd(C \wedge P)(S₂CNMe₂)] with HgI₂ affords the complex [Pd(C \wedge P)(S₂CNMe₂)HgI(μ-I)]₂ (**9**) similar to the complexes **3–6**; by contrast the reaction of [Pd(C \wedge P)(S₂C-R)] (R = NMe₂, OEt₂) with HgBr₂ leads to the corresponding dinuclear complexes [PdBr(S₂C-R)(μ-C \wedge P)HgBr] [R = NMe₂ (**10**), OEt (**11**)] with the didentate C \wedge P cyclometalating ligand, –CH₂-C₆H₄-P(*o*-tolyl)₂-C,P (resulting from the C–H activation of the P(*o*-tolyl)₃) acting in an unprecedented bridging mode. Compound **4** (C₂₄H₂₆HgI₂NPtS₂) crystallizes in the triclinic system, space group *P*1: *a* = 9.5755(11) Å, *b* = 11.1754(12) Å, *c* = 14.504(2) Å, α = 84.826(5)°, β = 81.611(7)°, γ = 68.606(9)°, *V* = 1428.5(3) Å³, and *Z* = 1. Compound **11**·0.5 HgBr₂·C₂H₄Cl₂ (C₂₄H₂₅Br₂HgOPdS₂·0.5 HgBr₂·C₂H₄Cl₂) crystallizes in the monoclinic system, space group *P*2₁/*c*: *a* = 15.571(2) Å, *b* = 10.7425(10) Å, *c* = 19.655(2) Å, β = 94.741(12)°, *V* = 3276.5(5) Å³, and *Z* = 4.

Introduction

Metal–metal bonding in heteronuclear complexes containing d⁸ and d¹⁰ metal ions has been known for some years.¹ We have developed chemistry for Pt^{II} and Ag^I using mono- or dinuclear anionic pentahalophenyl complexes of Pt(II) as Lewis bases,² and, more recently, heteronuclear Pt→Hg complexes obtained from this kind of Pt(II) substrates have also been reported.³

The ability of mercury to form heterodimetallic complexes with transition metal complex fragments is well-known.⁴ Some of these products have been prepared by reaction of HgX₂ (X = Cl, Br, I) with d⁸ transition metals,^{5–13} and the resulting complexes can be divided into those with a covalent metal–metal bond^{5–9} (type I) and those with a metal to metal donor–acceptor bond^{10–13} (type II). Reactions of HgX₂ (X = Cl, Br,

I) with organoplatinum(II) compounds have been found to proceed differently: In some cases, oxidative addition of HgX₂ to Pt^{II} renders compounds containing a Pt^{IV}–Hg covalent bond, as seems to occur in the reaction of *cis*-[PtMe₂(Ph₂Me₂phen)] with HgX₂ (X = Cl, Br, I),⁹ and in other cases the oxidative addition process is followed by a reductive elimination so that the platinum substrate acts as an alkylating agent toward the Hg center, as happens in the reactions of *cis*-[PtMe₂(PPhMe₂)] and *cis*-[PtMe₂(bpy)] with HgCl₂.¹⁴ As far as we know, no examples of Pt^{II}→HgX₂ adducts have yet been prepared by reacting the Pt substrate with HgX₂. In comparison to the situation with platinum, the chemistry of Pd^{II} derivatives with HgX₂ is much less developed.¹⁵

We have previously reported the reactivity of [Pt{CH₂-C₆H₄-P(*o*-tolyl)₂-κC,P}(S₂C-R)] (R = NMe₂, OEt) toward halogens (Cl₂, Br₂, I₂) to give the Pt(IV) compounds [Pt{CH₂-C₆H₄-P(*o*-tolyl)₂-κC,P}(S₂C-R)X₂] (R = NMe₂, OEt; X = Cl, Br, I) as a result of the oxidative addition of X₂ to the Pt(II) substrates.¹⁶ Since Hg(II) salts are able to add oxidatively to d⁸ metal fragments affording heteronuclear complexes containing metal–metal bonds, we have extended this work to the study of the reactivity of such mononuclear Pt(II) complexes [Pt{CH₂-C₆H₄-P(*o*-tolyl)₂-κC,P}(S₂C-R)] (R = NMe₂, OEt) toward HgX₂ (X = Br, I) and additionally to a study of similar Pd(II) complexes. As a result of this work, we report here the synthesis, structural characterization, and NMR studies of new mixed Pt–Hg and Pd–Hg complexes.

[⊗] Abstract published in *Advance ACS Abstracts*, December 1, 1997.

- (1) (a) Coffey, E.; Lewis, J.; Nyholm, R. S. *J. Chem. Soc.* **1964**, 1741. (b) Kuyper, J.; Vrieze, K. *J. Organomet. Chem.* **1976**, *107*, 129.
- (2) (a) Usón, R.; Forniés, J. *Adv. Organomet. Chem.* **1988**, *28*, 219. (b) Usón, R.; Forniés, J. *Inorg. Chim. Acta* **1992**, *198–200*, 165.
- (3) Usón, R.; Forniés, J.; Falvello, L. R.; Ara, I.; Usón, I. *Inorg. Chim. Acta* **1993**, *212*, 105.
- (4) Gade, L. H. *Angew. Chem., Int. Ed. Engl.* **1993**, *32*, 24.
- (5) Brotherton, P. D.; Raston, C. L.; White, A. H.; Wild, S. B. *J. Chem. Soc., Dalton Trans.* **1976**, 1799.
- (6) Tiripicchio, A.; Lahoz, F. J.; Oro, L. A.; Pinillos, M. T. *J. Chem. Soc., Chem. Commun.* **1984**, 936.
- (7) Einstein, F. W. B.; Yan, X.; Zhang, X.; Sutton, D. *J. Organomet. Chem.* **1992**, *439*, 221.
- (8) Brekau, U.; Werner, H. *Organometallics* **1990**, *9*, 1067.
- (9) Kuyper, J. *Inorg. Chem.* **1978**, *17*, 1458.
- (10) Faraone, F.; Schiavo, S. L.; Bruno, G.; Bombieri, G. *J. Chem. Soc., Chem. Commun.* **1984**, 6.
- (11) Faraone, F.; Tresoldi, G.; Loprete, G. A. *J. Chem. Soc., Dalton Trans.* **1979**, 933.
- (12) Nowell, I. W.; Russell, D. R. *J. Chem. Soc., Dalton Trans.* **1972**, 2393.
- (13) Faraone, F.; Bruno, G.; Tresoldi, G.; Faraone, G.; Bombieri, G. *J. Chem. Soc., Dalton Trans.* **1981**, 1651.

- (14) (a) Cross, R. J.; Wardle, R. *J. Chem. Soc. A* **1970**, 840. (b) Jawad, J. K.; Puddephatt, R. J. *J. Chem. Soc., Chem. Commun.* **1977**, 892. (c) Jawad, J. K.; Puddephatt, R. J. *Inorg. Chim. Acta* **1978**, *31*, L391.
- (15) Barr, R. M.; Goldstein, M.; Hairs, N. D.; McPartlin, M.; Markwell, A. J. *J. Chem. Soc., Chem. Commun.* **1974**, 221.
- (16) Forniés, J.; Martín, A.; Navarro, R.; Sicilia, V.; Villarroya, P. *Organometallics* **1996**, *15*, 1826.

Experimental Section

Elemental analyses were performed on a Perkin-Elmer 240-B micro-analyzer. IR spectra were recorded on a Perkin-Elmer 599 spectrophotometer (Nujol mulls between polyethylene plates in the range 200–4000 cm⁻¹). NMR spectra were recorded on either a Varian XL-200 or a Varian Unity 300 NMR spectrometer using the standard references. [Pd(OOCCH₃)₂]₂,¹⁷ [Pt{CH₂-C₆H₄-P(*o*-tolyl)₂-κC,P}(S₂CNMe₂)] (1)¹⁶ and [Pt{CH₂-C₆H₄-P(*o*-tolyl)₂-κC,P}(S₂COEt)] (2)¹⁶ were prepared as described elsewhere.

Safety Note. *Caution!* Perchlorate salts are potentially explosive. Only small amounts of material should be prepared, and these should be handled with great caution.

[Pd{CH₂-C₆H₄-P(*o*-tolyl)₂-κC,P}(μ-OOCCH₃)₂]₂.¹⁸ A mixture of [Pd(OOCCH₃)₂] (1.216 g, 5.42 mmol) and P(*o*-tolyl)₃ (1.649 g, 5.42 mmol) was refluxed in Me₂CO (45 mL) for 1 h. The dark green precipitate was filtered off and recrystallized from CH₂Cl₂/Et₂O (yield: 2.012 g, 79%).

[Pd{CH₂-C₆H₄-P(*o*-tolyl)₂-κC,P}(μ-Cl)]₂. To a solution of [Pd{CH₂-C₆H₄-P(*o*-tolyl)₂-κC,P}(μ-OOCCH₃)₂] (0.119 g, 2.38 mmol) in MeOH/CH₂Cl₂ (25:25 mL) was added LiCl (0.202 g, 4.77 mmol), and a dark green solid precipitated immediately. The solid was filtered off, washed with Et₂O, and dried in vacuo (yield: 1.06 g, 99.7%). IR data (cm⁻¹): C₂AP, 460 (vs), 470 (vs), 513 (s), 523 (vs), 560 (vs), 581 (vs), 753 (vs, br), 1568 (w), 1583 (m), 1590 (m); ν(Pd-Cl), 247 (s), 289 (s). Anal. Calcd for C₄₂H₄₀Pd₂Cl₂: C, 56.65; H, 4.53. Found: C, 56.34; H, 4.17.

[Pt{CH₂-C₆H₄-P(*o*-tolyl)₂-κC,P}(S₂CNMe₂)HgX(μ-X)]₂ (X = Br (3), I(4)). X = Br (3). To a pale yellow solution of compound 1 (0.2 g, 0.32 mmol) in CH₂Cl₂ (15 mL) was added HgBr₂ (0.116 g, 0.32 mmol), and the color of the solution turned orange immediately. The mixture was stirred for 10 min; then, the solvent was evaporated to dryness, and *n*-hexane (20 mL) was added to the residue (yield: 0.275 g, 87%). IR data (cm⁻¹): C₂AP, 456 (s), 474 (s), 488 (m), 504 (m), 528 (s), 562 (m), 586 (s), 758 (s), 774 (s), 1584 (w), 1595 (w); -S₂CNMe₂, 1554 (vs) (ν(C-N)), 968 (m) (ν(C-S)). ¹H NMR: C₂AP, 3.94 (s, 2H) (²J_{Pt-H} = 85.30 Hz, 75.80 Hz) (-CH₂-Pt), 2.37 (s), 2.61 (s) (CH₃-C₆H₄), 6.8–7.6 (m) (C₆H₄); -S₂CNMe₂, 3.33 (s), 3.34 (s). Anal. Calcd for Br₄C₄₈H₅₂Hg₂N₂P₂S₄: C, 29.44; H, 2.68; N, 1.43. Found: C, 29.25; H, 2.64; N, 1.42.

X = I (4). Compound 1 (0.151 g, 0.24 mmol) and HgI₂ (0.111 g, 0.24 mmol) in CH₂Cl₂ (25 mL) were reacted for 40 min. The solution was filtered and evaporated to dryness, whereupon addition of *n*-pentane (20 mL) gave compound 4 as an orange solid (yield: 0.228 g, 87%). IR data (cm⁻¹): C₂AP, 456 (s), 473 (s), 486 (s), 503 (m), 528 (s), 562 (s), 585 (s), 756 (s), 762 (s), 773 (s), 1584 (w), 1592 (w); -S₂CNMe₂, 1552 (vs) (ν(C-N)), 969 (m) (ν(C-S)). ¹H NMR: C₂AP, 3.88 (s, 2H) (²J_{Pt-H} = 95.20 Hz, 70.34 Hz) (-CH₂-Pt), 2.37 (s), 2.64 (s) (CH₃-C₆H₄), 6.8–7.8 (m) (C₆H₄); -S₂CNMe₂, 3.32 (s), 3.37 (s). Anal. Calcd for C₄₈H₅₂Hg₂I₂N₂P₂S₄: C, 26.86; H, 2.44; N, 1.31. Found: C, 26.73; H, 2.39; N, 1.29.

[Pt{CH₂-C₆H₄-P(*o*-tolyl)₂-κC,P}(S₂COEt)HgX(μ-X)]₂ (X = Br (5), I(6)). X = Br (5). To a yellow solution of compound 2 (0.218 g, 0.35 mmol) in CH₂Cl₂ (25 mL) was added HgBr₂ (0.127 g, 0.35 mmol); the color of the solution turned to a brighter yellow. The mixture was stirred for 5 min and the solution evaporated to dryness. Addition of *n*-pentane (30 mL) to the residue afforded compound 5 as a yellow solid (yield: 0.29 g, 84%). IR data (cm⁻¹): C₂AP, 464 (m), 482 (m), 492 (m), 510 (w), 529 (s), 569 (m), 597 (s), 758 (s), 779 (s), 1579 (w), 1597 (w), 1602 (w); -S₂COEt, 1022 (vs), 1126 (s), 1275 (vs). ¹H NMR: C₂AP, 3.98 (s, 2H) (²J_{Pt-H} = 103.44 Hz, 72.41 Hz) (-CH₂-Pt), 2.39 (s), 2.65 (s) (CH₃-C₆H₄), 6.8–7.6 (m) (C₆H₄); -S₂COEt, 4.70 (q), 1.53 (t) (³J_{H-H} = 7.10 Hz). Anal. Calcd for Br₄C₄₈H₅₀Hg₂O₂P₂S₄: C, 29.41; H, 2.57. Found: C, 29.12; H, 2.47.

X = I (6). Complex 6 was prepared in a similar way. Compound 2 (0.135 g, 0.22 mmol) and HgI₂ (0.099 g, 0.22 mmol) were mixed in CH₂Cl₂/OEt₂ (10/40 mL) for 30 min. After filtration the resulting

orange solution was evaporated to dryness. Addition of *n*-pentane (30 mL) to the residue afforded compound 6 as an orange solid (yield: 0.162 g, 70%). IR data (cm⁻¹): C₂AP, 450 (w), 479 (m), 490 (m), 512 (w), 526 (s), 568 (m), 599 (s), 756 (s), 788 (s), 1574 (m), 1605 (m); -S₂COEt, 1024 (vs), 1135 (s), 1278 (vs). ¹H NMR: C₂AP, 3.71 (s, 2H) (²J_{Pt-H} = 97.30 Hz, 85.10 Hz) (-CH₂-Pt), 2.40 (s), 2.69 (s) (CH₃-C₆H₄), 6.8–7.6 (m) (C₆H₄); -S₂COEt, 4.64 (q), 1.49 (t) (³J_{H-H} = 7.10 Hz). Anal. Calcd for C₄₈H₅₀I₂Hg₂O₂P₂S₄: C, 26.84; H, 2.35. Found: C, 26.64; H, 2.28.

[Pd{CH₂-C₆H₄-P(*o*-tolyl)₂-κC,P}(S₂CNMe₂)] (7). To a stirred suspension of [Pd{CH₂-C₆H₄-P(*o*-tolyl)₂-κC,P}(μ-Cl)]₂ (0.475 g, 0.53 mmol) in tetrahydrofuran (THF, 30 mL) was added AgClO₄ (0.221 g, 1.07 mmol), and the mixture was stirred at room temperature for 15 min. The AgCl precipitated was filtered off, and the resulting solution was evaporated almost to dryness. The residue was treated with 30 mL of methanol, and the addition of NaS₂CNMe₂·2H₂O (0.191 g, 1.07 mmol) to the solution gave a yellow solid 7, which was filtered off and washed with MeOH and *n*-pentane (yield: 0.534 g, 94%). IR data (cm⁻¹): C₂AP, 445 (s), 461 (s), 468 (s), 480 (s), 509 (s), 525 (s), 558 (s), 578 (s), 754 (vs), 761 (vs), 1581 (m); -S₂CNMe₂, 1531 (vs) (ν(C-N)), 974 (s) (ν(C-S)). ¹H NMR: C₂AP, 3.38 (s) (-CH₂-Pd), 2.44 (s), 2.74 (s) (CH₃-C₆H₄), 6.7–7.4 (m) (C₆H₄); -S₂CNMe₂, 3.29 (s), 3.34 (s). Anal. Calcd for C₂₄H₂₆NPPdS₂: C, 54.39; H, 4.94; N, 2.64. Found: C, 53.95; H, 4.33; N, 2.88.

[Pd{CH₂-C₆H₄-P(*o*-tolyl)₂-κC,P}(S₂COEt)] (8). To the solution resulting from the treatment of [Pd{CH₂-C₆H₄-P(*o*-tolyl)₂-κC,P}(μ-Cl)]₂ (0.469 g, 0.53 mmol) with AgClO₄ (0.218 g, 1.05 mmol), in THF (20 mL), after elimination of the AgCl, was added K₂S₂COEt (0.169 g, 1.05 mmol), and the mixture was stirred for 15 min at room temperature. After filtration the solution was evaporated to dryness, *n*-hexane (25 mL) was added, and the solution was concentrated to a small volume (5 mL). The resulting suspension was cooled at 5 °C to afford a yellow solid which was recrystallized from CH₂Cl₂/*n*-hexane (-20 °C), compound 8 (yield: 0.4253 g, 76%). IR data (cm⁻¹): C₂AP, 461 (s), 470 (s), 478 (s), 511 (s), 527 (s), 559 (s), 579 (s), 752 (vs), 761 (vs), 1583 (m), 1591 (w); -S₂COEt, 1030 (s), 1203 (s). ¹H NMR: C₂AP, 3.48 (s) (-CH₂-Pd), 2.39 (s), 2.66 (s) (CH₃-C₆H₄), 6.6–7.4 (m) (C₆H₄); -S₂COEt, 4.56 (q), 1.39 (t) (³J_{H-H} = 7.20 Hz). Anal. Calcd for C₂₄H₂₅OPPdS₂: C, 54.20; H, 4.75. Found: C, 54.49; H, 4.76.

[Pd{CH₂-C₆H₄-P(*o*-tolyl)₂-κC,P}(S₂CNMe₂)HgI(μ-I)] (9). To a yellow solution of compound 7 (0.216 g, 0.41 mmol) in CH₂Cl₂ (25 mL) was added an equimolar amount of HgI₂ (0.185 g, 0.41 mmol) and OEt₂ (45 mL). The mixture was stirred for 1 h, and the resulting yellow solid 9 was filtered off and dried in vacuo. An additional amount of compound 9 was obtained from the resulting solution by evaporation almost to dryness and addition of *n*-pentane (20 mL) to the residue (total yield: 0.36 g, 90%). IR data (cm⁻¹): C₂AP, 451 (s), 471 (s), 481 (s), 500 (m), 520 (s), 559 (m), 584 (m), 751 (vs), 758 (vs), 1584 (m), 1591 (m); -S₂CNMe₂, 1549 (vs) (ν(C-N)), 971 (vs) (ν(C-S)). ¹H NMR: C₂AP, 3.59 (s) (-CH₂-Pd), 2.50 (s), 2.70 (s) (CH₃-C₆H₄), 6.8–7.5 (m) (C₆H₄); -S₂CNMe₂, 3.44 (s, 6H). Anal. Calcd for C₄₈H₅₂Hg₂I₂N₂P₂S₄: C, 29.28; H, 2.66; N, 1.42. Found: C, 29.33; H, 2.59; N, 1.47.

[PdBr(S₂CNMe₂){μ-P(*o*-tolyl)₂-C₆H₄-CH₂}-HgBr] (10). To a yellow solution of compound 7 (0.15 g, 0.28 mmol) in CH₂Cl₂ (25 mL) at -25 °C was added an equimolar amount of HgBr₂ (0.102 g, 0.28 mmol), whereupon the color of the solution turned orange. After 40 min of stirring, the mixture was filtered, and the resulting solution was evaporated to dryness. Addition of Et₂O (-20 °C) to the residue rendered a yellow solid, 10 (yield: 0.195 g, 77%). IR data (cm⁻¹): C₂AP, 442 (m), 461 (s), 478 (s), 501 (m), 522 (m), 537 (s), 551 (m), 568 (s), 754 (vs), 1591 (m); -S₂CNMe₂, 1554 (vs) (ν(C-N)), 970 (vs) (ν(C-S)). ¹H NMR: C₂AP, 3.43 (d, 1H) 3.72 (d, 1H, ²J_{H-H} = 9.1 Hz) (-CH₂-Pd), 1.52 (s), 1.76 (s) (CH₃-C₆H₄), 6.8–7.6 (m, 11H), 9.12 (d, 1H) (C₆H₄); -S₂CNMe₂, 3.12 (s), 3.28 (s). Anal. Calcd for Br₂C₂₄H₂₆HgNPPdS₂: C, 32.37; H, 2.94; N, 1.57. Found: C, 32.17; H, 2.90; N, 1.62.

[PdBr(S₂COEt){μ-P(*o*-tolyl)₂-C₆H₄-CH₂}-HgBr] (11). To a solution of compound 8 (0.125 g, 0.24 mmol) in CHCl₃ (30 mL) at -30 °C was added HgBr₂ (0.17 g, 0.47 mmol); the color of the solution turned orange. After 2 h, the mixture was filtered through celite and the filtrate was evaporated almost to dryness. Addition of cold *n*-pentane (-20 °C) to the residue afforded compound 11 as a yellow

(17) Heyn, B.; Hipler, B.; Kreisel, G.; Schreer, H.; Walther, D. *Angewandte Synthesechemie*; Springer-Verlag: Berlin, 1986; p 142.

(18) This complex was prepared recently by Herrmann in a different way: Herrmann, W. A.; Brossmer, Ch.; Öfele, K.; Reisinger, C.-P.; Priermeier, T.; Beller, M.; Fischer, H. *Angew. Chem., Int. Ed. Engl.* 1995, 34, 1844.

Table 1. Crystallographic Data for $[\text{Pt}\{\text{CH}_2\text{-C}_6\text{H}_4\text{P}(o\text{-tolyl})_2\}\kappa\text{C}, \text{P}\}\{\text{S}_2\text{CNMe}_2\}\text{HgI}(\mu\text{-I})_2$ (**4**) and $[\text{PdBr}(\text{S}_2\text{COEt})\{\mu\text{-P}(o\text{-tolyl})_2\}\kappa\text{C}, \text{P}\}\{\text{S}_2\text{CNMe}_2\}\text{HgBr}_2 \cdot \text{C}_2\text{H}_4\text{Cl}_2$ (**11**·0.5 $\text{HgBr}_2 \cdot \text{C}_2\text{H}_4\text{Cl}_2$)

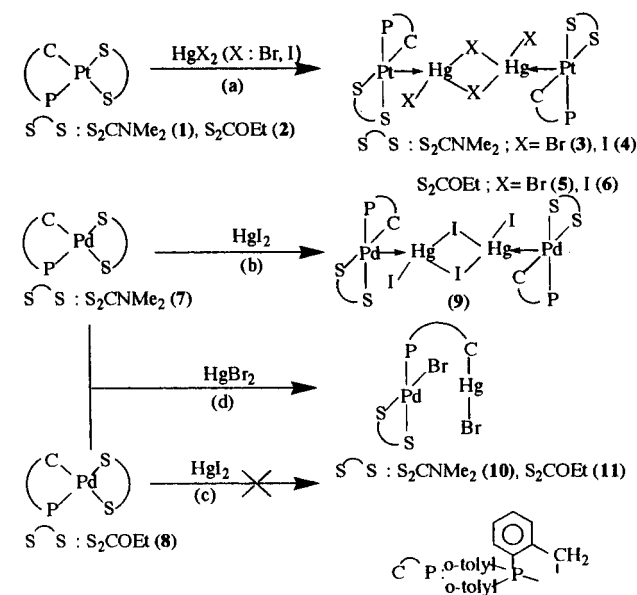
	4	11 ·0.5 $\text{HgBr}_2 \cdot \text{C}_2\text{H}_4\text{Cl}_2$
empirical formula	$\text{C}_{48}\text{H}_{52}\text{Hg}_2\text{I}_4\text{N}_2\text{P}_2\text{S}_4$	$\text{C}_{24}\text{H}_{25}\text{Br}_2\text{HgOPPdS}_2 \cdot 0.5 \text{HgBr}_2 \cdot \text{C}_2\text{H}_4\text{Cl}_2$
fw	2146.13	1348.72
temp (K)	273(1)	143(1)
wavelength (Å)		0.710 73
space group	$P\bar{1}$	$P2_1/c$
unit cell dimensions		
<i>a</i> (Å)	9.5755(11)	15.571(2)
<i>b</i> (Å)	11.1754(12)	10.7425(10)
<i>c</i> (Å)	14.504(2)	19.655(2)
α (deg)	84.826(5)	90
β (deg)	81.611(7)	94.741(12)
γ (deg)	68.606(9)	90
vol (Å ³)	1428.5(3)	3276.5(5)
Z	1	4
ρ_{calc} (Mg/m ³)	2.50	2.37
abs coeff (mm ⁻¹)	12.64	11.58
final <i>R</i> indices ^a	$R = 0.0351$, [$I > 2\sigma(I)$] $R_w = 0.0371$	$R = 0.0410$, $R_w = 0.0848$
<i>R</i> indices ^a (all data)	$R = 0.0839$, $R_w = 0.0501$	$R = 0.0735$, $R_w = 0.0964$

^a $R = \sum ||F_o| - |F_c|| / \sum |F_o|$; $R_w = [\sum w(|F_o| - |F_c|)^2 / \sum w|F_o|^2]^{1/2}$; $R_w^2 = [\sum [w(F_o^2 - F_c^2)]^2 / \sum w(F_o^2)^2]^{1/2}$.

solid (yield: 0.159 g, 76%). IR data (cm⁻¹): C \wedge P, 458 (s), 478 (s), 501 (m), 521 (s), 534 (s), 560 (s), 580 (s), 755 (vs, sh), 1563 (m), 1589 (m); S_2COEt , 1021 (vs, br), 1234 (vs, br). ¹H NMR (218 K): C \wedge P, 3.38 (d, 1H), 3.76 (d, 1H, ²J_{H-H} = 10.8 Hz) ($\text{CH}_2\text{-Pd}$), 1.54 (s), 1.76 (s) ($\text{CH}_3\text{-C}_6\text{H}_4$), 6.7–7.6 (m, 11H), 9.04 (d, 1H) (C_6H_4); S_2COEt , 4.65 (q), 1.42 (t) (³J_{H-H} = 7.10 Hz). Anal. Calcd for $\text{Br}_2\text{C}_2\text{H}_5\text{HgOPPdS}_2$: C, 32.34; H, 2.83. Found: C, 31.98; H, 2.81.

Crystal Structure Determination of $[\text{Pt}\{\text{CH}_2\text{-C}_6\text{H}_4\text{P}(o\text{-tolyl})_2\}\kappa\text{C}, \text{P}\}\{\text{S}_2\text{CNMe}_2\}\text{HgI}(\mu\text{-I})_2$ (4**).** Important crystal data and data collection parameters for complex **4** are listed in Table 1. A parallelepiped-shaped crystal mounted on the tip of a glass fiber with epoxy cement was used for geometric and intensity data collection. All diffraction measurements were made at room temperature on a Siemens STOE/AED2 four circle diffractometer. Lattice dimensions and type were determined by routine procedures and verified by oscillation photography. Cell constants were refined from 2 θ values of 70 reflections including Friedel pairs ($17.3 < 2\theta < 35.7^\circ$). Diffracted intensities were measured in a unique hemisphere of reciprocal space for $4.0 < 2\theta < 50.0^\circ$ by ω scans. During intensity data collection, three monitor reflections were measured at regular intervals, and they did not vary appreciably in intensity during the course of data collection. A measured absorption correction was applied on the basis of complete Ψ -scans of reflections with diffractometer angle χ near 90° . The structure of compound **4** was solved by direct methods and developed and refined in a series of alternating difference Fourier maps and least squares analyses using all data and the program package SHELXTL-PLUS.^{19a} All non-hydrogen atoms were refined anisotropically. All hydrogen atoms were included in calculated positions and refined as riding atoms (C–H, 0.96 Å; $U = 0.0917 \text{ \AA}^3$). Final difference electron density maps showed no peaks above 1 e \AA^{-3} (largest peak, 0.84 e \AA^{-3} ; largest difference hole, -0.77 e \AA^{-3}). Residuals and other final refinement parameters are listed in Table 1. Residuals are defined in ref 19a.

Crystal Structure Determination of $[\text{PdBr}(\text{S}_2\text{COEt})\{\mu\text{-P}(o\text{-tolyl})_2\}\kappa\text{C}, \text{P}\}\{\text{S}_2\text{CNMe}_2\}\text{HgBr}_2 \cdot \text{C}_2\text{H}_4\text{Cl}_2$ (11**·0.5 $\text{HgBr}_2 \cdot \text{C}_2\text{H}_4\text{Cl}_2$).** Crystal data and other details of the structure analysis are presented in Table 1. A crystal of compound **11**·0.5 $\text{HgBr}_2 \cdot \text{C}_2\text{H}_4\text{Cl}_2$ was mounted at the end of a quartz fiber and glued in place with epoxy adhesive. All diffraction measurements were made at 143(1) K on an Enraf-Nonius

Scheme 1

CAD4 diffractometer, using graphite monochromated Mo K_{α} X-radiation. Unit cell dimensions were determined from 25 centered reflections in the range $23.6 < 2\theta < 31.8^\circ$. Diffracted intensities were measured in a unique quadrant of reciprocal space for $4.0 < 2\theta < 50.0^\circ$ by ω/θ scans. Three check reflections remeasured after every 3 h showed no decay of the crystal over the period of data collection. An absorption correction was applied on the basis of 555 azimuthal scan data (maximum and minimum transmission coefficients were 0.854 and 0.435). Lorentz and polarization corrections were applied. The structure was solved by Patterson and Fourier methods. All non-hydrogen atoms were assigned anisotropic displacement parameters and refined without positional constraints. The hydrogen atoms were constrained to idealized geometries and assigned isotropic displacement parameters 1.2 times the U_{iso} value of their parent carbon atoms (1.5 times for the methyl hydrogen atoms). The carbon atoms of the 1,2-dichloroethane solvent molecule are disordered over two sets of positions (partial occupancy 0.5) and were refined with a common set of anisotropic thermal parameters. Full-matrix least squares refinement of this model against F^2 converged to final residuals given in Table 1. Final difference electron density maps showed three peaks above 1 e \AA^{-3} (1.24, 1.19, and 1.06 e \AA^{-3} ; largest difference hole, -1.22) lying within 1.06 \AA of the mercury atoms. Least squares calculations were carried out using the program SHELXL-93.^{19b} Residuals are defined in ref 19b.

Results and Discussion

Reactivity of Complexes $[\text{Pt}\{\text{CH}_2\text{-C}_6\text{H}_4\text{P}(o\text{-tolyl})_2\}\kappa\text{C}, \text{P}\}\{\text{S}_2\text{CR}\}]$ [$\text{R} = \text{NMe}_2$ (1**), OEt (**2**)] toward HgX_2 ($\text{X} = \text{Br}, \text{I}$).** The reactions of $[\text{Pt}\{\text{CH}_2\text{-C}_6\text{H}_4\text{P}(o\text{-tolyl})_2\}\kappa\text{C}, \text{P}\}\{\text{S}_2\text{CR}\}]$ ($\text{R} = \text{NMe}_2$ (**1**), OEt (**2**)) with HgX_2 ($\text{X} = \text{Br}, \text{I}$) (1:1 molar ratio) in dichloromethane afford the tetranuclear complexes $[\text{Pt}\{\text{CH}_2\text{-C}_6\text{H}_4\text{P}(o\text{-tolyl})_2\}\kappa\text{C}, \text{P}\}\{\text{S}_2\text{CR}\}\text{HgX}(\mu\text{-X})_2]$ in high yields as air stable solids (Scheme 1a).

The IR spectra of complexes **3** and **4** show several absorptions corresponding to the $\text{Me}_2\text{NCS}_2^-$ ligand in a bidentate coordination mode²⁰ (see Experimental Section). The values of the $\nu_{\text{C-N}}$ (CN) [1554 cm^{-1} (**3**), 1552 cm^{-1} (**4**)] suggest a pronounced degree of C–N double bonding, even more so than in the starting complex (1543 cm^{-1}). The IR spectra of complexes **5** and **6** also show the typical absorptions of the EtOCS_2^- group.²⁰

Figure 1 shows the molecular structure of compound **4** with the atom numbering scheme. General crystallographic information is collected in Table 1. Relevant bond distances and angles are listed in Table 2.

(19) (a) SHELXTL-PLUS Software Package for the Determination of Crystal Structures, Release 4.0; Siemens Analytical X-ray Instruments, Inc.: Madison, WI, 1990. (b) Sheldrick, G. M. SHELXL-93, a program for crystal structure determination; University of Göttingen: Göttingen, Germany, 1993.

(20) Coucouvanis, D. *Progress in Inorganic Chemistry*; John Wiley & Sons: New York, 1979; Vol. 26, p 424.

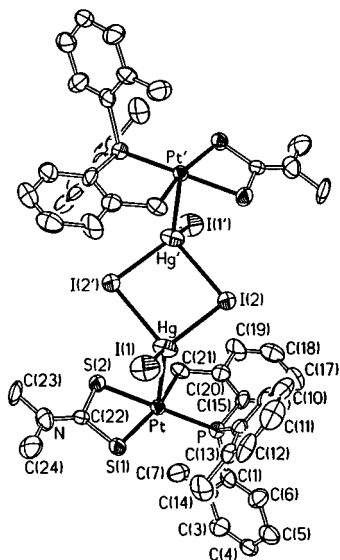


Figure 1. Drawing of the crystal structure of $[\text{Pt}\{\text{CH}_2\text{-C}_6\text{H}_4\text{P}(o\text{-tolyl})_2\text{-}\kappa\text{C,P}\}(\text{S}_2\text{CNMe}_2)\text{HgI}(\mu\text{-I})_2]_2$ (**4**), showing the atom labeling scheme. Atoms are represented by their 50% probability ellipsoids.

Table 2. Selected Bond Lengths (Å) and Angles (deg) for $[\text{Pt}\{\text{CH}_2\text{-C}_6\text{H}_4\text{P}(o\text{-tolyl})_2\text{-}\kappa\text{C,P}\}(\text{S}_2\text{CNMe}_2)\text{HgI}(\mu\text{-I})_2]_2$ (**4**)

Pt—Hg	2.768(1)	Pt—C(21)	2.081(14)
Pt—P	2.246(4)	Pt—S(1)	2.413(4)
Pt—S(2)	2.341(5)	C(22)—N	1.315(21)
C(22)—S(1)	1.707(14)	C(22)—S(2)	1.733(14)
Hg—I(1)	2.661(1)	Hg—I(2)	2.766(2)
Hg—I(2')	3.041(1)		
S(1)—Pt—S(2)	73.9(1)	C(22)—N—C(24)	122.1(13)
S(1)—Pt—P	107.5(1)	Pt—Hg—I(1)	113.8(1)
P—Pt—C(21)	84.6(4)	Pt—Hg—I(2)	112.4(1)
S(2)—Pt—C(21)	94.0(4)	Pt—Hg—I(2')	109.5(1)
S(1)—C(22)—N	125.5(1)	I(1)—Hg—I(2)	122.7(1)
S(2)—C(22)—N	122.2(10)	I(1)—Hg—I(2')	105.0(1)
C(22)—N—C(23)	121.9(13)	I(2)—Hg—I(2')	89.5(1)
Hg—I(2)—Hg'	90.5(1)		

The tetranuclear complex **4** can be regarded as being formed by two “ $\text{Pt}\{\text{CH}_2\text{-C}_6\text{H}_4\text{P}(o\text{-tolyl})_2\text{-}\kappa\text{C,P}\}(\text{S}_2\text{CNMe}_2)\text{HgI}_2$ ” units bridged by two I atoms and related to each other by a center of symmetry.

As can be seen, each unit contains one unsupported Pt—Hg bond. In each unit the five-coordinated Pt atom is located at the center of the base of a square pyramid with the Hg atom in the apical position. The angle between the Pt—Hg vector and the perpendicular to the Pt basal plane [Pt, C(21), P, S(1), S(2)] is 9.19° .²¹

Bond distances and angles corresponding to the “ $\text{Pt}\{\text{CH}_2\text{-C}_6\text{H}_4\text{P}(o\text{-tolyl})_2\text{-}\kappa\text{C,P}\}(\text{S}_2\text{CNMe}_2)$ ” fragment are similar to those observed in the Pt(II) complex which is used as starting material.¹⁶

The Pt—Hg distance [2.768(1) Å] and the geometry around the Pt center are similar to those observed in $[\{2,6\text{-}(\text{Me}_2\text{NCH}_2)_2\text{-C}_6\text{H}_3\}\text{Pt}(\mu\text{-}\{p\text{-tol}\}\text{NC}(\text{H})\text{N}(\text{Pr})\}\text{HgBrCl}]$ [2.8331(7) Å],²² *trans*- $[(\text{CH}_3\text{NH}_2)_2\text{Pt}(1,5\text{-diMeC}^-)_2\text{Hg}](\text{NO}_3)_2 \cdot 0.5 \text{H}_2\text{O}$ [2.765(1) Å],²³ *trans*- $[(\text{CH}_3\text{NH}_2)_2\text{Pt}(1\text{-MeC}^-)_2\text{HgCl}(\text{NO}_3)]$ [2.835(1) Å],²³ and *trans*- $[(\text{CH}_3\text{NH}_2)_2\text{Pt}(1\text{-MeC}^-)_2\text{Hg}](\text{NO}_3)_2$ [2.785(1) Å],²³ for which the Pt—Hg interaction has been described as a Pt→Hg donor bond with both metals in a formal oxidation state of 2. In contrast, the Pt—Hg distance is clearly different from the distances observed in mixed Pt—Hg compounds displaying a

covalent bond: $[(2\text{-Me}_2\text{NCH}_2\text{-C}_6\text{H}_4)_2(\mu\text{-MeCO}_2)\text{PtHg}(\text{O}_2\text{CMe})]$, 2.513(1) Å;²⁴ $[(\text{PPh}_3)_2\text{R-Pt-Hg-R}]$, 2.637(1) Å;^{25a} $[\text{PhCH}[\text{HgPt}(\text{Ph}_3\text{P})_2\text{Br}]\text{COOC}_{10}\text{H}_{19}]$, 2.499 Å;^{25b} $[\text{N}(\text{CH}_2\text{CH}_2\text{PPh}_2)_3\text{Pt}(\text{HgMe})\text{BPh}_4]$, 2.531(1) Å;^{25c} $[\text{PtCl}(\text{HgMe})(\text{dmphen})(Z\text{-MeO}_2\text{-CCH}=\text{CHCO}_2\text{Me})]$, 2.558(1) Å.^{25d}

It is noteworthy that, in complex **4**, the Pt→Hg bond is not supported by any bridging ligand, especially considering that the basic Pt complex $[\text{Pt}\{\text{CH}_2\text{-C}_6\text{H}_4\text{P}(o\text{-tolyl})_2\text{-}\kappa\text{C,P}\}(\text{S}_2\text{CNMe}_2)]$ used as starting material contains two S atoms with pairs of electrons capable of forming a Hg—S bond. Mercury, furthermore, has a well-known affinity for sulfur.²⁶ The absence of bridging ligands between the Pt and Hg centers makes compound **4** different from the other complexes exhibiting Pt^{II} to Hg^{II} donor bonds.^{22,23}

From the point of view of the Hg(II), the complex can be considered as a dimer of stoichiometry $[\text{HgII}(\mu\text{-I})_2]$, L being the complex $[\text{Pt}\{\text{CH}_2\text{-C}_6\text{H}_4\text{P}(o\text{-tolyl})_2\text{-}\kappa\text{C,P}\}(\text{S}_2\text{CNMe}_2)]$ with the Pt acting as the donor atom. Each Hg atom is located in a very distorted tetrahedral environment, the Hg—I terminal distance [2.661(1) Å] being shorter than the Hg—I bridging ones, which are in turn very different from each other [Hg—I(2), 2.766(2) Å, Hg—I(2'), 3.041(1) Å], in keeping with the structures of other $[\text{LHgX}(\mu\text{-X})_2]$ complexes.^{27,28} The Hg—I(2)—Hg—I(2') fragment is planar and the angles I(2)—Hg—I(2') and Hg—I(2)—Hg' are nearly 90° .

Although the literature contains numerous reports of 1:1 complexes of mercuric halides with neutral ligands such as $[\text{HgX}(\text{Me}_3\text{SiCH}_2\text{SeMe})(\mu\text{-X})_2]$ (X = Cl, Br, I),^{27a} $[\text{HgI}(\text{Ph}_3\text{PC}_5\text{H}_4)(\mu\text{-I})_2]$,^{27b} $[\text{HgCl}(\text{PBU}_3)(\mu\text{-Cl})_2]$,^{28a} or $[\text{Ph}_3\text{PCHCO}_6\text{H}_5\text{-HgX}_2]_2$ (X = Cl, I)^{28d} showing discrete centrosymmetric halogen bridged dimeric structures, to our knowledge, there is none in which the neutral ligand is a metal complex with the metal center acting as donor atom, as in this case.

In agreement with the molecular symmetry observed in the crystal, the $^{31}\text{P}\{\text{H}\}$ NMR spectra of complexes **3–6** (see Table 3) show only one singlet at about 25 ppm with the corresponding ¹⁹⁵Pt satellites. The P—Pt coupling constants in these complexes are smaller than those of the starting materials (see Table 3) in the range of about 200–400 Hz.

The ¹H NMR spectra of complexes **3–6** in CDCl₃ at room temperature (20 °C) also confirm the equivalence of the two halves of the molecule in each case. These spectra show a common pattern due to the cyclometalated group “ $\text{Pt}\{\text{CH}_2\text{-C}_6\text{H}_4\text{P}(o\text{-tolyl})_2\text{-}\kappa\text{C,P}\}$ ” (see Experimental Section): (a) The CH₃ groups of the *o*-tolylphosphine appear as two singlets indicating

(21) Nardelli, M. *Comput. Chem.* **1983**, *7*, 95.

(22) van der Ploeg, A. F. M. J.; van Koten, G.; Vrieze, K.; Spek, A. L.; Duisenberg, A. J. M. *Organometallics* **1982**, *1*, 1066.

(23) Krumm, M.; Zangrando, E.; Randaccio, L.; Menzer, S.; Danzmann, A.; Holtherrich, D.; Lippert, B. *Inorg. Chem.* **1993**, *32*, 2183.

(24) (a) van der Ploeg, A. F. M. J.; van Koten, G.; Vrieze, K.; Spek, A. L.; Duisenberg, A. J. M. *J. Chem. Soc., Chem. Commun.* **1980**, 469. (b) van der Ploeg, A. F. M. J.; van Koten, G.; Vrieze, K.; Spek, A. L. *Inorg. Chem.* **1982**, *21*, 2014.

(25) (a) Rossell, O.; Seco, M.; Torra, I.; Solans, X.; Font-Altava, M. *J. Organomet. Chem.* **1984**, *270*, C63. (b) Suleimanov, G. Z.; Bashilov, V. V.; Musaev, A. A.; Sokolov, V. I.; Reutov, O. A. *J. Organomet. Chem.* **1980**, *202*, C61. (c) Ghilardi, C. A.; Midollini, S.; Moneti, S.; Orlandini, A.; Scapacci, G.; Dakternieks, D. *J. Chem. Soc., Chem. Commun.* **1989**, 1686. (d) Cucciolito, E.; Giordano, F.; Panunzi, A.; Rufo, F.; de Felice, V. *J. Chem. Soc., Dalton Trans.* **1993**, 3421.

(26) (a) Christou, G.; Folting, K.; Huffman, J. C. *Polyhedron* **1984**, *3*, 1247. (b) Bond, A. M.; Colton, R.; Hollenkamp, A. F.; Hoskins, B. F.; McGregor, K. *J. Am. Chem. Soc.* **1987**, *109*, 1969.

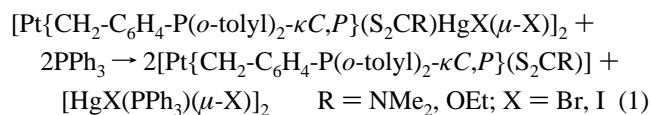
(27) (a) Chadha, R. K.; Drake, J. E.; McManus, N. T.; Mislankar, A. *Can. J. Chem.* **1987**, *65*, 2305. (b) Baenziger, N. C.; Flynn, R. M.; Swenson, D. C. *Acta Crystallogr.* **1978**, *B34*, 2300.

(28) (a) Bell, N. A.; Goldstein, M.; Jones, T.; Nowell, I. W. *Inorg. Chim. Acta* **1980**, *43*, 87. (b) van Enkevort, W. J. P.; Beurskens, P. T.; Menger, E. M.; Bosman, W. P. *Cryst. Struct. Commun.* **1977**, *6*, 417. (c) Castineiras, A.; Arquero, A.; Masaguer, J. R.; Martínez-Carrera, S.; García Blanco, S. *Anorg. Allg. Chem.* **1986**, *539*, 219. (d) Kalyanasundari, M.; Panchanatheswaran, K.; Robinson, W. T.; Wen, H. *J. Organomet. Chem.* **1995**, *491*, 103.

their inequivalence; (b) the signals corresponding to the CH₂–Pt group are isochronous, showing however different values of $^2J_{195\text{Pt-H}}$; (c) the aromatic hydrogens give several multiplets between 6.5 and 7.8 ppm. The main difference observed with respect to the starting complex is the δ value of the CH₂–Pt signal together with the Pt–H coupling constant.

Square-pyramidal compounds containing Pt^{II}→Hg^{II} donor bonds (type II) have been proposed as intermediates in the formation of species with covalent Pt–Hg bonds (type I).²⁴ However, we have not observed the subsequent formation of type I complexes from compounds **3–6** (type II).

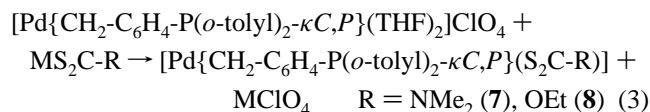
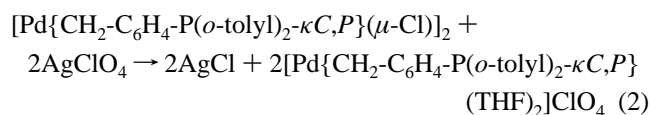
The reactions of compounds **3–6** with PPh₃ in 1:2 molar ratio afford the starting Pt(II) complexes [Pt{CH₂–C₆H₄–P(*o*-tolyl)₂– κ C,*P*}(S₂CR)] [R = NMe₂ (**1**), OEt (**2**)] as a result of the cleavage of the Pt^{II}→Hg^{II} bond rather than of the dihalogen bridging system (eq 1).



The reactivity of the platinum(II) complexes [Pt{CH₂–C₆H₄–P(*o*-tolyl)₂– κ C,*P*}(S₂CR)] [R = NMe₂ (**1**), OEt (**2**)] toward HgX₂ prompted us to study the reactions of the analogous palladium(II) complexes with the aim of preparing the corresponding derivatives with Pd→Hg bonds.

Synthesis and Characterization of [Pd{CH₂–C₆H₄–P(*o*-tolyl)₂– κ C,*P*}(S₂CR)] (R = NMe₂ (7**), OEt (**8**)).** These compounds have been prepared similarly to the previously reported platinum analogues.¹⁶

Solutions resulting from the reaction of [Pd{CH₂–C₆H₄–P(*o*-tolyl)₂– κ C,*P*}(μ-Cl)]₂ with AgClO₄ (1:2 molar ratio) in THF at room temperature, presumably containing the [Pd{CH₂–C₆H₄–P(*o*-tolyl)₂– κ C,*P*}(THF)₂]ClO₄ species, react with equimolar amounts of sodium dimethyldithiocarbamate (NaS₂CNMe₂·2H₂O) and potassium ethylxanthate (KS₂COEt) to give the mononuclear complexes [Pd{CH₂–C₆H₄–P(*o*-tolyl)₂– κ C,*P*}(S₂CNMe₂)] (**7**) and [Pd{CH₂–C₆H₄–P(*o*-tolyl)₂– κ C,*P*}(S₂COEt)] (**8**) as air stable solids (see Experimental Section; eqs 2 and 3).



The similarities of the IR and ¹H NMR spectra of compounds **7** and **8** to those of the analogous Pt complexes [Pt{CH₂–C₆H₄–P(*o*-tolyl)₂– κ C,*P*}(S₂CR)] [R = NMe₂ (**1**), OEt (**2**)] suggest a similar structure for all of them, consisting of square-planar mononuclear complexes with bidentate chelating ligands. As in the Pt derivatives **1** and **2**, the hindered rotation of the P–C_{ipso} bonds at room temperature causes the inequivalence of the two CH₃ groups of the *o*-tolylphosphine. The ΔG^\ddagger values at the coalescence temperature of the methyl resonances, for the P–C_{ipso} bond rotation process in complexes **7** ($\Delta G^\ddagger_{319\text{K}} = 64.2$ KJ mol⁻¹) and **8** ($\Delta G^\ddagger_{313\text{K}} = 63.2$ KJ mol⁻¹) have been calculated using the approximation to Eyring's equation,²⁹ and they are very similar to the values found for the analogous platinum derivatives **1** and **2**.

Table 3. ³¹P{¹H} NMR^a Data for Complexes **1–11**

complex	δP (ppm)	$^1J_{\text{Pt-P}}$ (Hz)	$\Delta^1J_{\text{Pt-P}}$ (Hz)
[Pt(C \wedge P)(S ₂ CNMe ₂)] (1)	24.70 (s)	3969.4	
[Pt(C \wedge P)(S ₂ COEt)] (2)	23.73 (s)	4083.8	
[Pt(C \wedge P)(S ₂ CNMe ₂)HgBr(μ -Br)] ₂ (3)	26.06 (s)	3594.93	374.5 ^c
[Pt(C \wedge P)(S ₂ CNMe ₂)HgI(μ -I)] ₂ (4)	25.69 (s)	3681.10	288.3 ^c
[Pt(C \wedge P)(S ₂ COEt)HgBr(μ -Br)] ₂ (5)	25.16 (s)	3745.80	338.0 ^d
[Pt(C \wedge P)(S ₂ COEt)HgI(μ -I)] ₂ (6)	24.63 (s)	3862.75	221.0 ^d
[Pd(C \wedge P)(S ₂ CNMe ₂)] (7)	35.58 (s)		
[Pd(C \wedge P)(S ₂ COEt)] (8)	35.93 (s)		
[Pd(C \wedge P)(S ₂ CNMe ₂)HgI(μ -I)] ₂ (9)	36.76 (s)		
[PdBr(S ₂ CNMe ₂)(μ -P \wedge C)HgBr] (10) ^b	20.24 (s)		
[PdBr(S ₂ COEt)(μ -P \wedge C)HgBr] (11) ^b	20.71 (s)		

^a C \wedge P, CH₂–C₆H₄–P(*o*-tolyl)₂– κ C,*P*; external reference H₃PO₄, 85%; CDCl₃; room temperature. ^b 218 K. ^c $\Delta^1J_{\text{Pt-P}} = ^1J_{\text{Pt-P}}(\mathbf{1}) - ^1J_{\text{Pt-P}}$. ^d $\Delta^1J_{\text{Pt-P}} = ^1J_{\text{Pt-P}}(\mathbf{2}) - ^1J_{\text{Pt-P}}$.

Reactivity of [Pd{CH₂–C₆H₄–P(*o*-tolyl)₂– κ C,*P*}(S₂CR)] [R = NMe₂ (7**), OEt (**8**)] toward HgX₂ (X = Br, I).** The reactions of [Pd{CH₂–C₆H₄–P(*o*-tolyl)₂– κ C,*P*}(S₂CR)] (R = NMe₂ (**7**), OEt (**8**)) with HgX₂ (X = Br, I) proceed differently depending on the nature of X and the S₂CR⁻ ligands.

[Pd{CH₂–C₆H₄–P(*o*-tolyl)₂– κ C,*P*}(S₂CNMe₂)] (**7**) reacts with HgI₂ at room temperature in a 1:1 molar ratio to give [Pd{CH₂–C₆H₄–P(*o*-tolyl)₂– κ C,*P*}(S₂CNMe₂)HgI(μ -I)]₂ (**9**) in a very high yield (Scheme 1b), whereas the xanthate complex [Pd{CH₂–C₆H₄–P(*o*-tolyl)₂– κ C,*P*}(S₂COEt)] (**8**) does not react with HgI₂ under similar conditions or even when the reactants are refluxed in diethyl ether for several hours (Scheme 1c). The structure of **9** has been assigned on the bases of the similarities of its IR and ³¹P{¹H} and ¹H NMR spectra with its platinum-containing analogues, [Pt{CH₂–C₆H₄–P(*o*-tolyl)₂– κ C,*P*}(S₂CNMe₂)HgBr(μ -Br)]₂ (**3**) and [Pt{CH₂–C₆H₄–P(*o*-tolyl)₂– κ C,*P*}(S₂CNMe₂)HgI(μ -I)]₂ (**4**).

HgBr₂ reacts with both complexes **7** and **8**, giving similar complexes although different from the one obtained in the reaction with HgI₂. Treatment of dichloromethane solutions of [Pd{CH₂–C₆H₄–P(*o*-tolyl)₂– κ C,*P*}(S₂CR)] [R = NMe₂ (**7**), OEt (**8**)] with HgBr₂ at low temperature (–25 °C) affords the air stable solids [PdBr(S₂CNMe₂){ μ -P(*o*-tolyl)₂–C₆H₄–CH₂-}HgBr] (**10**) and [PdBr(S₂COEt){ μ -P(*o*-tolyl)₂–C₆H₄–CH₂-}HgBr] (**11**) in high yields (Scheme 1d). As can be seen in Figure 2, compounds **10** and **11** are the result of transmetalation processes in which Pd–Br and C–Hg bonds are formed. These reactions have to be performed at low temperature [–25 °C and –30 °C] in order to avoid the formation of an unidentified byproduct which appears as an impurity ($\delta P = 42$ ppm) in products **10** and **11** when the reactions are carried out at room temperature.

The geometry of the binuclear palladium–mercury complex [PdBr(S₂COEt){ μ -P(*o*-tolyl)₂–C₆H₄–CH₂-}HgBr] (**11**), as determined by X-ray diffraction studies, is illustrated in Figure 2 together with the atomic numbering scheme. General crystallographic information is collected in Table 1. Relevant bond distances and angles are listed in Table 4.

As can be seen, the molecule contains one palladium and one mercury atom bridged by the bidentate “P(*o*-tolyl)₂–C₆H₄–CH₂–” group, the Pd–Hg distance being 3.098(1) Å.

The palladium atom is located in a distorted square-planar environment formed by one bromine, two sulfur atoms of the ethylxanthate ligand, and the P of the bidentate bridging group; the S(1) atom is 0.159 Å away from the best plane²¹ defined by Pd, Br(1), S(1), S(2), and P. The angles around the palladium center between *cis* ligand bonds range from 74.9(1) to 97.6(1)°, distortion which can be mainly due to the small bite angle

(29) Günther, H. *NMR Spectroscopy: An Introduction*; John Wiley & Sons: Chichester, U.K., 1980.

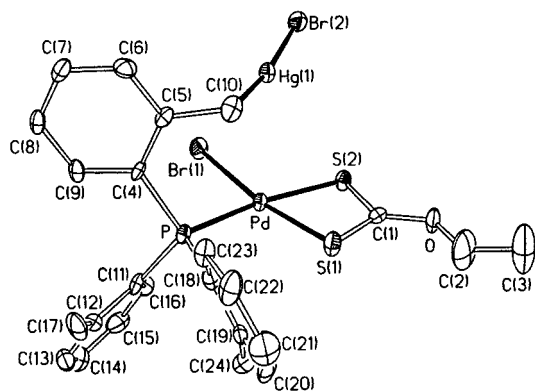


Figure 2. Drawing of the crystal structure of [PdBr(S₂COEt){μ-P(*o*-tolyl)₂-C₆H₄-CH₂}HgBr] (**11**), showing the atom labeling scheme. Atoms are represented by their 50% probability ellipsoids.

Table 4. Selected Bond Lengths (Å) and Angles (deg) for [PdBr(S₂COEt){μ-P(*o*-tolyl)₂-C₆H₄-CH₂}HgBr]·0.5 HgBr₂·C₂H₄Cl₂ (**11**·0.5HgBr₂·C₂H₄Cl₂)

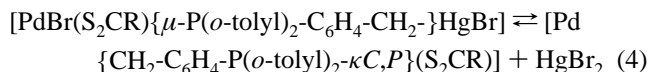
Pd—Br(1)	2.454(1)	Pd—P	2.305(2)
Pd—S(1)	2.288(3)	Pd—S(2)	2.389(2)
Pd—Hg	3.098(1)	Hg—Br(2)	2.460(1)
Hg—C(10)	2.106(10)	S(1)—C(1)	1.693(10)
S(2)—C(1)	1.706(10)	O—C(1)	1.299(11)
O—C(2)	1.489(14)	C(2)—C(3)	1.35(2)
S(1)—Pd—P	94.93(9)	S(1)—Pd—S(2)	74.90(9)
Br(1)—Pd—P	92.58(7)	S(2)—Pd—Br(1)	97.62(7)
C(5)—C(10)—Hg(1)	109.5(6)	C(10)—Hg(1)—Br(2)	171.1(3)
S(1)—C(1)—S(2)	113.7(5)	S(1)—C(1)—O	125.8(8)
S(2)—C(1)—O	120.5(7)	C(1)—O—C(2)	116.5(9)

of the chelate xanthate ligand (74.1°).³⁰ Pd—S distances are different, with Pd—S(2) [2.389(2) Å] longer than Pd—S(1) [2.288(3) Å], probably because of the higher *trans* influence of the P ligand compared to the bromide. The Pd—P distance [2.305(2) Å] is slightly longer than that observed in the complexes [Pd{CH₂-C₆H₄-P(*o*-tolyl)₂-κC,P}(μ-OOCCH₃)₂]¹⁸ and [Pt{CH₂-C₆H₄-P(*o*-tolyl)₂-κC,P}(S₂CNMe₂)]¹⁶ in which the C^P ligand acts as a chelate.

The xanthate ligand is essentially planar and almost coplanar with the Pd coordination plane (dihedral angle 6.3°). The C—S bond lengths [1.693(10), 1.706(10) Å] are very similar to those observed in other complexes with chelating xanthate ligands,³¹ but the C—O distance [1.489(14) Å] is longer than those normally observed in this type of complexes and is as long as a typical C—O single bond.³¹

The Hg atom is located at 3.098(1) Å from the Pd atom and is close to the perpendicular to the Pd coordination plane; the angle between the perpendicular to the palladium coordination plane and the Pd—Hg vector is 17.5°. The Hg is coordinated to a Br and to the C donor atom of the bridging “P(*o*-tolyl)₂-C₆H₄-CH₂—” group in almost a linear mode [C(10)—Hg—Br(2) = 171.1(3)°] as is usual for RHgX compounds.³² The Hg—Br^{5,27b} and the Hg—C^{3,25} distances are similar to those found in other organometallic Hg complexes.

The compound [PdBr(S₂COEt){μ-P(*o*-tolyl)₂-C₆H₄-CH₂}-HgBr] (**11**) crystallizes with 0.5 molecules of HgBr₂. The presence of HgBr₂ in the crystal can be explained in terms of the equilibrium represented in eq 4. The fact that complexes **10** and **11** dissociate in solution according to eq 4 is confirmed by the ³¹P{¹H} NMR data.

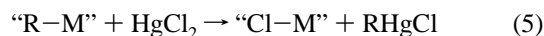


The ³¹P{¹H} NMR spectra of [PdBr(S₂CR){μ-P(*o*-tolyl)₂-C₆H₄-CH₂}HgBr] [R = NMe₂ (**10**), OEt (**11**)] at room temperature show in both cases two signals, one due to complex **10** or **11**, respectively, and the other corresponding to the starting material **7** or **8**, respectively.

The spectrum of complex **10** at −55 °C does not show the signal corresponding to the starting material, while the spectrum of complex **11** at −55 °C shows the two signals observed at room temperature. The disappearance of the signal due to the starting material (at −55 °C) requires that HgBr₂ be added to the above mentioned solution of **11**. All these facts suggest that complexes **10** and **11** dissociate in solution at room temperature (**10**) or even low temperature (**11**) (eq 4).

As can be seen from the ³¹P{¹H} NMR data (Table 3), the new disposition of the C^P group, which now acts as a bridge between the Pd and Hg atoms, leads to an important change in the position of the ³¹P signal (about 15 ppm) with respect to the cases in which this ligand acts as a chelate at the Pd center (complexes **7**–**9**). The new arrangement also causes important changes in the ¹H NMR spectrum, especially in the signals corresponding to the —CH₂— group, which appears as an AX system with a ²J_{H—H} close to 10 Hz, and also for those of CH₃—C₆H₄, which are shifted to lower δ by almost 1 ppm.

The formation of complexes **10** and **11** takes place as a result of a transmetalation process. Cleavage of platinum carbon σ bonds by electrophiles such as HgCl₂ have been observed previously.^{14b,c} These reactions result in alkyl or aryl transfer from the platinum substrate to mercury and the formation of organomercurials (eq 5).



In our case, although the cleavage of the Pd—C σ bond takes place, the bidentate nature of the C,P-cyclometalated ligand leads to the formation of Pd—Hg complexes with the ligand acting as a bridge between the two metal centers.

Dirhodium(II) compounds with metalated arylphosphines acting as bridges between the two metal centers have been reported, with the phosphines forming three-atom bridges.³³ The formation of a four-atom bridge between two metal centers is very rare due to the stability of the five-membered metallocycles, and as far as we know only one such compound —[(C₆F₅)(8-mq)Pd(μ-8-mq)Pd(C₆F₅)(phen)] (8-mq = 8-quinolylmethyl)—containing a C,N metalated ligand (8-mq) with a four-atom bridge has previously been reported.³⁴

The present results show the greater capacity of Pt(II), as compared to Pd(II), for the formation of donor—acceptor metal—metal bonds, as well as the predisposition of Hg to bond to carbon.

Acknowledgment. We thank the Dirección General de Enseñanza Superior (Spain) for financial support (Projects PB95-0003-CO2-01 and PB95-0792).

Supporting Information Available: For the crystal structure of **4**, full tables of crystallographic data, atomic coordinates, thermal parameters, and bond lengths and angles (5 pages). X-ray crystallographic files, in CIF format, for complex **11**·0.5HgBr₂·C₂H₄Cl₂ are available on the Internet only. Ordering and access information is given on any current masthead page.

(30) Usón, R.; Forniés, J.; Falvello, L. R.; Tomás, M.; Ara, I.; Usón, I. *Inorg. Chim. Acta* **1995**, *232*, 35.

(31) Orpen, G.; Brammer, L.; Allen, F. H.; Kennard, O.; Watson, D. G.; Taylor, R. *J. Chem. Soc., Dalton Trans.* **1989**, S1.

(32) Cotton, F. A.; Wilkinson, G. *Advanced Inorganic Chemistry*, 5th ed.; John Wiley & Sons: New York, 1988; p 618.

(33) Estevan, F.; González, G.; Lahuerta, P.; Martínez, M.; Peris, E.; van Eldik, R. *J. Chem. Soc., Dalton Trans.* **1996**, 1045.

(34) Forniés, J.; Navarro, R.; Sicilia, V.; Tomás, M. *Organometallics* **1990**, *9*, 2422.